

SUPPORTING INFORMATION FOR:
Establishing tungsten carbides as active catalysts for CO₂ hydrogenation

Pulse oxidation quantification of active sites for estimating turnover frequency (TOF):

$$TOF = \frac{F_{CO_2} * X}{n_{W_xC}}$$

Where F_{CO_2} is the inlet molar flow rate of CO₂, X is CO₂ conversion, and n_{W_xC} is the number of moles of W_xC, determined by pulse oxidation (found in Table 1). For active site quantification, we assume each WC site adsorbs and reacts with two oxygen molecules to form the passivation layer of tungsten oxides.

Supporting Figures and Tables:

Table S1. Median and average particle size of IWI and M catalysts carburized at 835 °C for 2 hours, 5 hours and 10 hours with reported standard deviations.

Catalyst	Median Particle Size (nm)	Average Particle Size (nm)
M 835 °C - 2hr	9.4 ± 7.5	12.4 ± 7.5
M 835 °C - 5hr	8.3 ± 8.1	10.9 ± 8.1
M 835 °C - 10hr	11.1 ± 8.4	12.9 ± 8.4
IWI 835 °C - 2hr	11.7 ± 6.7	12.3 ± 6.7
IWI 835 °C - 5hr	11.1 ± 7.0	11.7 ± 7.0
IWI 835 °C - 10hr	8.7 ± 4.6	9.1 ± 4.6

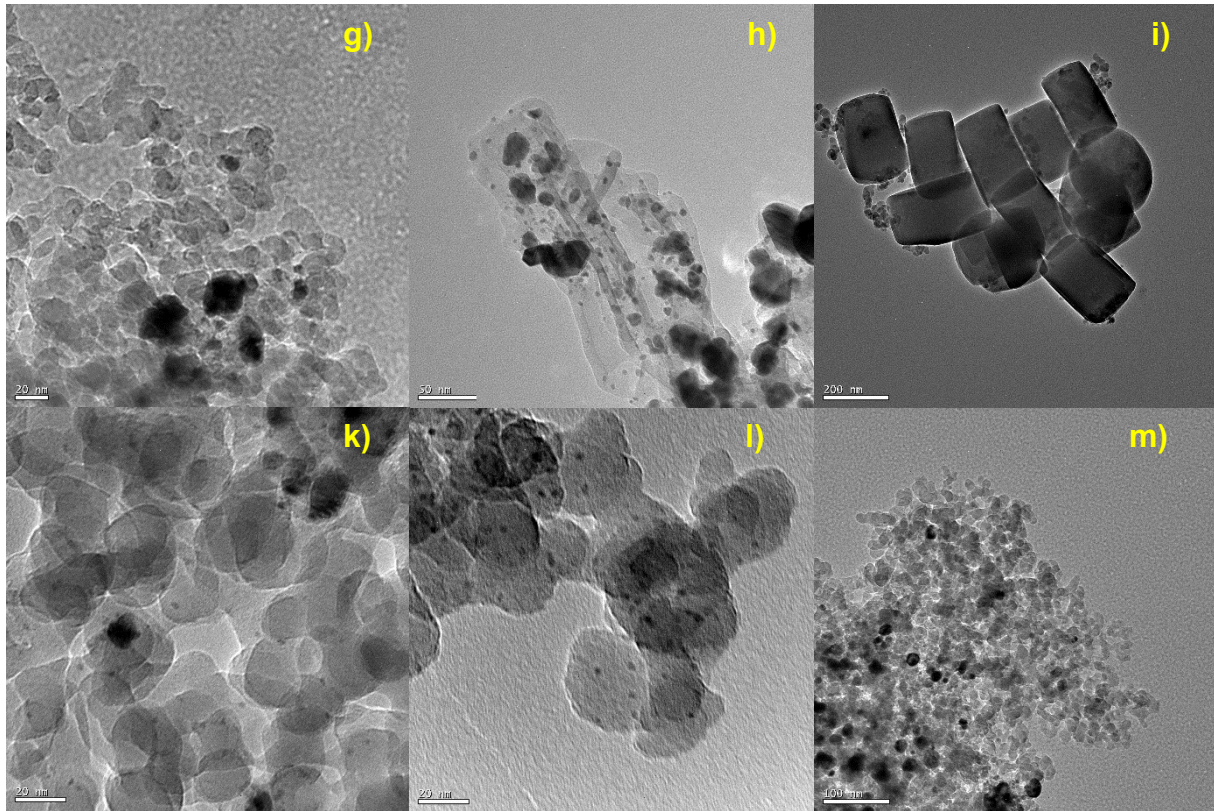
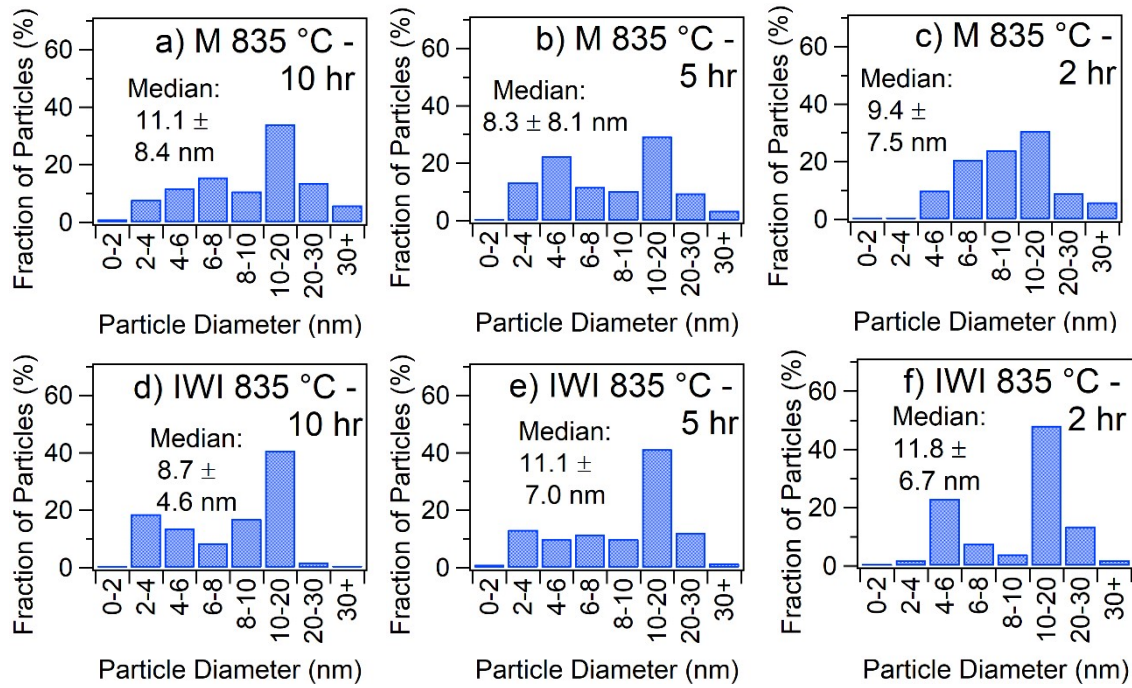


Figure S1. Particle size distributions of nano- W_xC (M) carburized at 835 °C for a) 10 hours, b) 5 hours, and c) 2 hours, and IWI W_xC carburized at 835 °C for d) 10 hours, e) 5 hours and f) 2 hours with corresponding TEM images (g-m).

Table S2. BET surface areas of IWI and M catalysts.

Catalyst	BET Surface Area (m ² /g)	
	IWI	M
Calcined at 550 °C	149	99
Carburized at 600 °C	128	1.7
Carburized at 835 °C	173	98
Carburized at 1000 °C	112	68

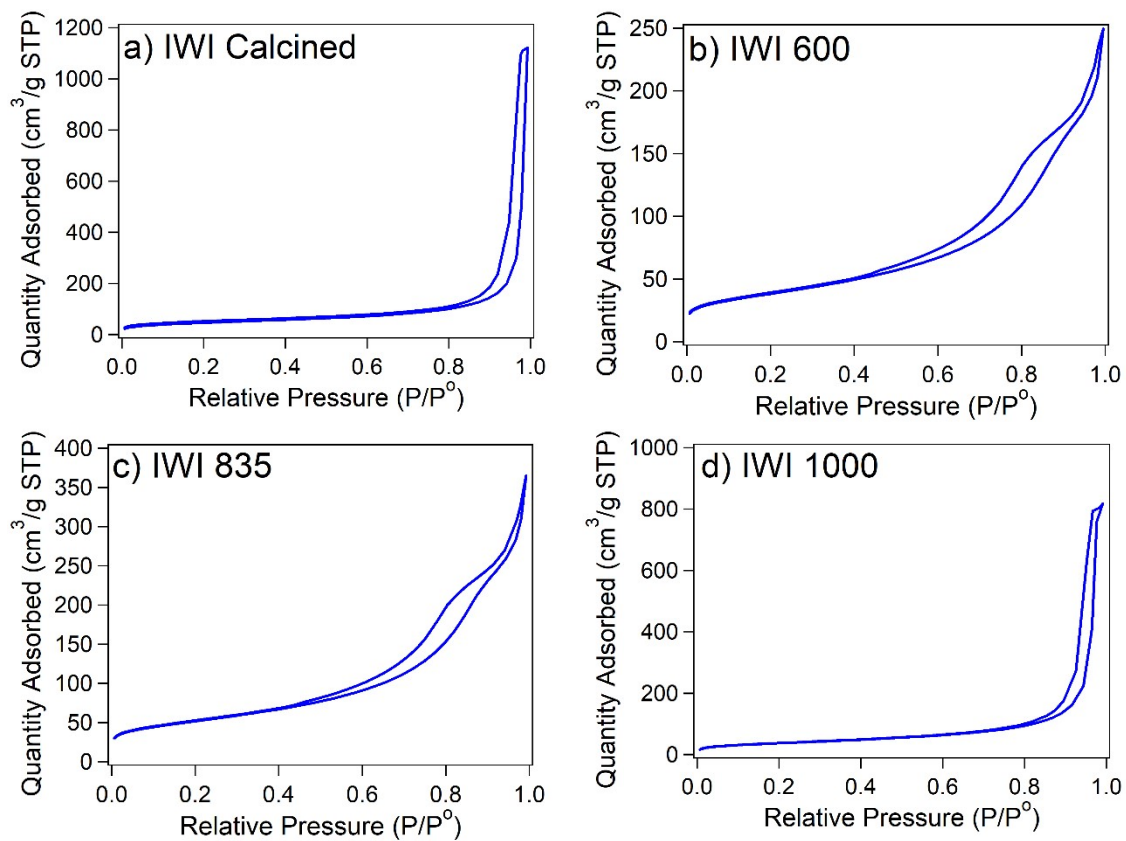


Figure S2. BET Isotherms of IWI catalysts. a) Calcined and b-d) carburized at each respective temperature.

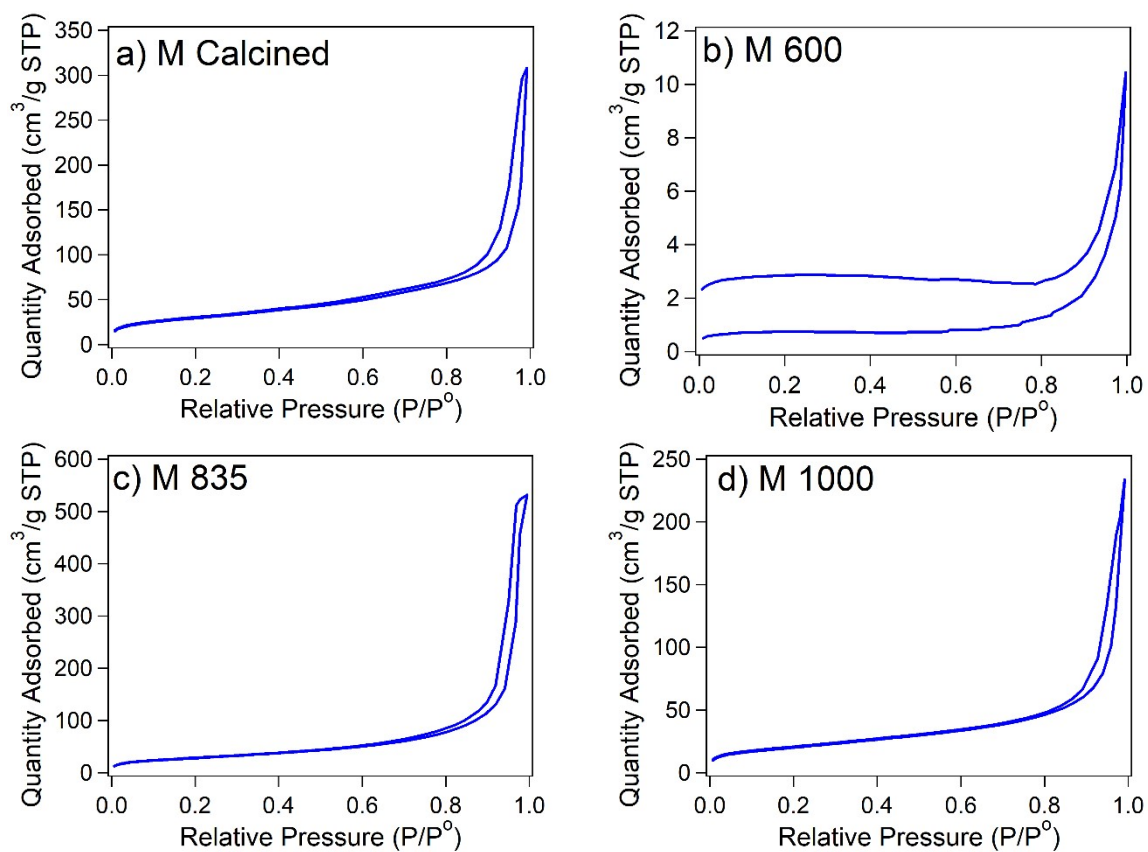


Figure S3. BET Isotherms of M catalysts. a) Calcined and b-d) carburized at each respective temperature.

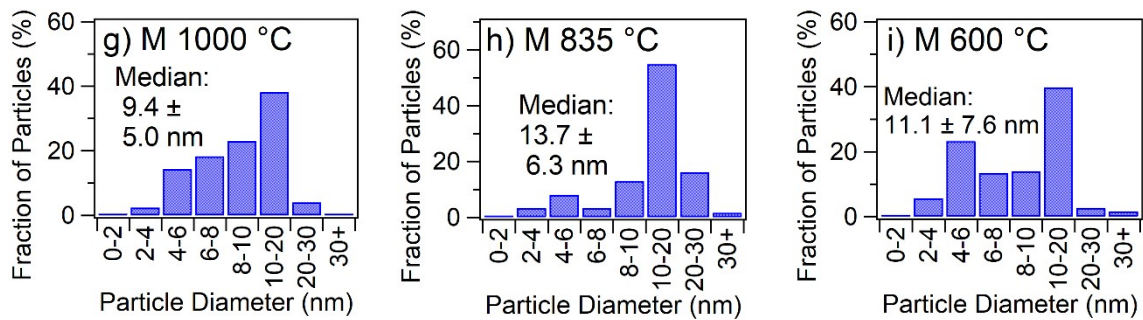
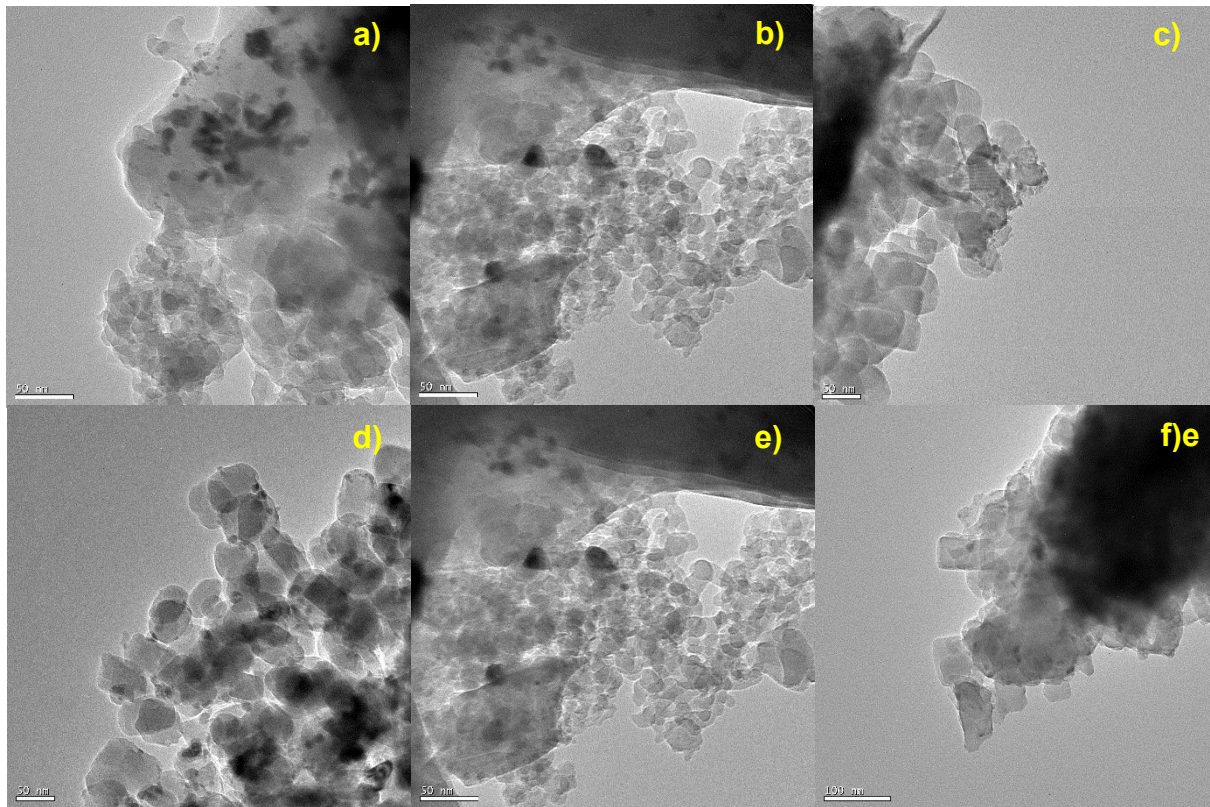


Figure S4. TEM images with 50 nm scale bar of nano- W_xC after 12 hrs on stream during RWGS, and carburized at a,d) 1000 °C, b,e) 835 °C, and c,f) 600 °C, with respective particle size distributions (g-i).

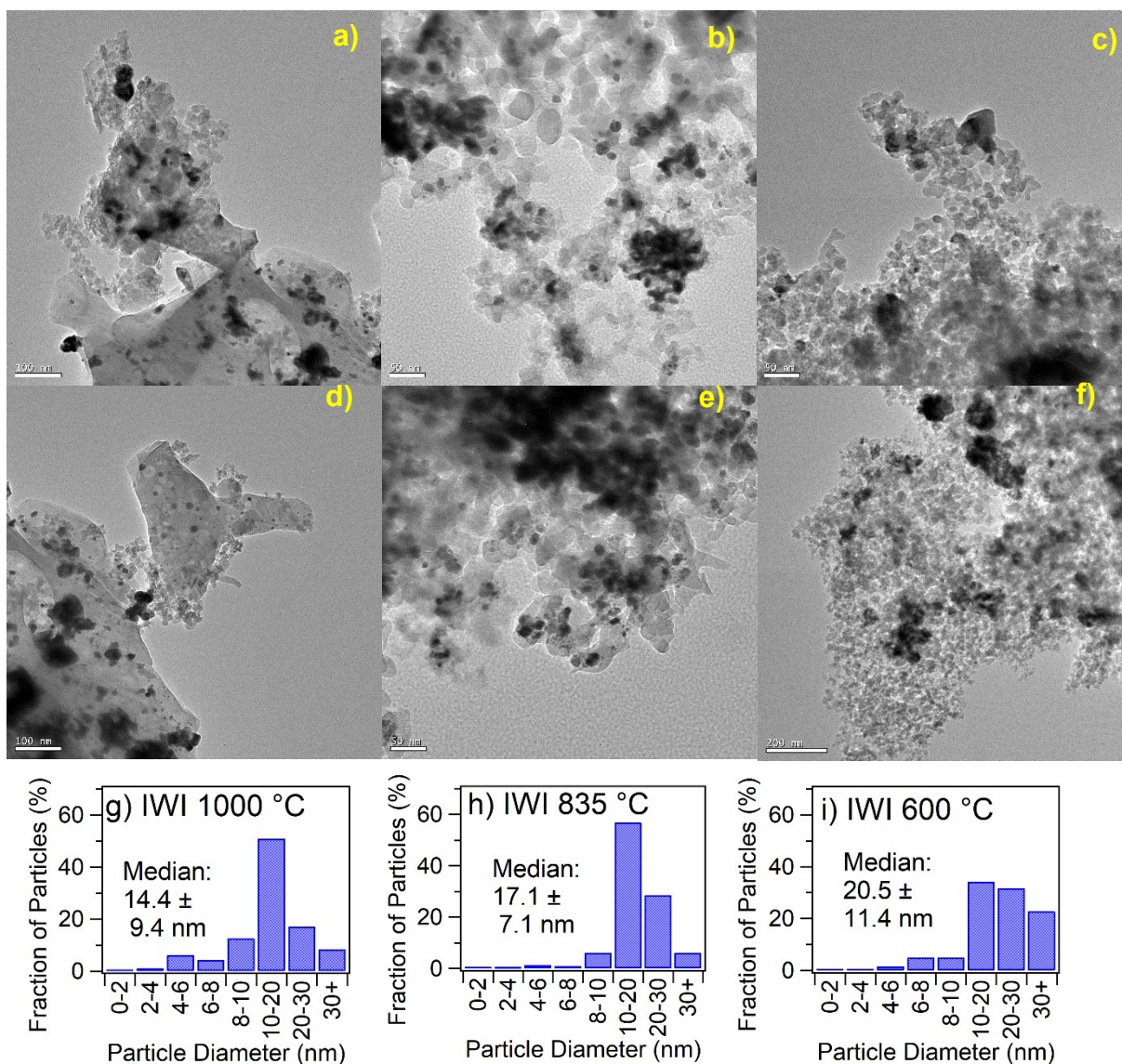


Figure S5. TEM images with 50 nm scale bar of IWI W_xC after 12 hrs on stream during RWGS, and carburized at a,d) 1000 °C, b,e) 835 °C, and c,f) 600 °C, and respective particle size distributions (g-i).

Table S3. Median particle size of IWI and M catalysts carburized at 600 °C, 835 °C, and 1000 °C with reported standard deviation for as-synthesized and post-RWGS catalysts.

Carburization Temperature (°C)	IWI Median Particle Size ± Std. Dev. (nm)		M Median Particle Size ± Std. Dev. (nm)	
	As-Synthesized	Post-RWGS	As-Synthesized	Post-RWGS
600	13.7 ± 5.8	20.5 ± 11.4	15.7 ± 8.4	11.1 ± 7.6
835	11.1 ± 7.0	17.1 ± 7.1	7.2 ± 6.1	13.7 ± 6.3
1000	13.0 ± 7.4	14.4 ± 9.4	6.7 ± 7.3	9.4 ± 5.0

Table S4. Cumulative quantities of adsorbed O₂ during pulse oxidation with 1% O₂/N₂.

Catalyst	Cumulative Quantity of O ₂ Adsorbed (μmol/g)
M 600	2.5
M 835	2.6
M 1000	2.7
IWI 600	2.7
IWI 835	6.4
IWI 1000	2.5

Table S5. ICP-MS Loadings of IWI and M catalysts carburized at 600 °C, 835 °C and 1000 °C.

Catalyst	Tungsten Weight Percent (%)	Sodium Weight Percent (%)
M 600 °C	6.2	8.0
M 835 °C	6.8	8.0
M 1000 °C	7.4	8.0
IWI 600 °C	6.2	0.02
IWI 835 °C	7.1	0.02
IWI 1000 °C	8.5	0.02

Table S6. Peak positions and FWHM for fit XPS spectra.

Component		IWI 600 °C	IWI 835 °C	IWI 1000 °C	M 600 °C	M 835 °C	M 1000 °C
W	Peak Position (eV)	31.0	31.2	30.3	30.8	30.3	30.9
	FWHM	0.8	1.0	1.3	0.9	1.1	1.3
W₂C	Peak Position (eV)	31.4	31.5	31.6	31.3	31.2	31.2
	FWHM	1.2	1.2	1.1	0.8	0.9	1.8
WC	Peak Position (eV)	31.8	32.3	32.5	31.9	31.8	32.0
	FWHM	0.8	1.2	0.8	1.2	0.8	1.1
WO₂	Peak Position (eV)	32.9	32.9	33.3	33.0	32.9	32.8
	FWHM	1.8	1.5	1.8	1.4	0.8	1.8
WO₃	Peak Position (eV)	35.6	35.6	36.2	35.2	35.2	35.3
	FWHM	2.0	2.0	2.0	1.8	2.0	2.0

Table S7. Selected catalysts for benchmarking catalytic performance of IWI and M W_xC catalysts. The asterisk (*) indicates this work.

Catalyst	T (°C)	P (MPa)	H ₂ :CO ₂ Ratio	GHSV (L/kg/s)	Conversion (%)	Carbon-based Selectivity (%)			CO Yield (%)	CO STY (μmol CO/gcat/s)	CO Production (kg CO/kgMetal/Day)
						CO	CH ₄	C ₂₊ Products			
M 600 *	350	2.1	3	7.5	2.5	96.5	3.5	0	2.4	1.80	29.0
M 835 *	350	2.1	3	7.5	4.9	99.2	0.8	0	4.9	3.62	58.3
M 1000 *	350	2.1	3	7.5	13.9	94.6	5	0.4	13.1	9.78	157.8
IWI 600 *	350	2.1	3	7.5	6.5	88	11.3	0.7	5.7	4.26	68.6
IWI 835 *	350	2.1	3	7.5	9.2	94.9	4.9	0.2	8.7	6.50	104.8
IWI 1000 *	350	2.1	3	7.5	5.9	86.3	12.9	0.8	5.1	3.79	61.1
WC ^[1]	300	2	3	1.0	8.8	89.9	10.1	0	7.9	1.18	8.9
WC ^[1]	350	2	3	1.0	24.3	88.0	12.0	0	21.4	3.18	24.1
KWC ^[1]	300	2	3	1.0	4.8	100.0	0.0	0	4.8	0.71	5.4
KWC ^[1]	350	2	3	1.0	20.3	98.1	1.9	0	19.9	2.96	22.4
NaWC	300	2	3	1.0	1.9	100.0	0.0	0	1.9	0.28	2.1
NaWC ^[1]	350	2	3	1.0	13.6	100.0	0.0	0	13.6	2.02	15.3
Cu-ZnO ^[1]	270	3	3	5.6	5.3	93.2	0.0	6.8	4.9	2.45	59.3
Cu/Mo ₂ C ^[2]	300	2	5	2.5	19.0	38.0	32.0	30.0	7.2	1.21	5.8
Ni/Mo ₂ C ^[2]	300	2	5	2.5	29.0	29.0	64.0	7.0	8.4	1.41	6.8
Co/Mo ₂ C ^[2]	300	2	5	2.5	31.0	19.0	37.0	44.0	5.9	0.99	4.8
Low T WGS Industrial Cu ^[3]	300	2.1	3	36.7	23.3	92.6	4.6	2.8	21.6	80.2	194.0
High T WGS Industrial FeCrOx	450	2.1	3	36.7	47.5	48.6	37.3	7.3	23.1	85.8	207.7
P-K-Mo ₂ C/γ-Al ₂ O ₃ ^[3]	300	2.1	3	36.7	1.2	99.2	0.8	0.0	1.2	4.3	52.9
P-K-Mo ₂ C/γ-Al ₂ O ₃ ^[3]	450	2.1	3	36.7	26.8	99.3	0.3	0.4	26.6	99.1	1219.0
P-K-Mo ₂ C/γ-Al ₂ O ₃ ^[3]	450	2.1	3	18.3	33.1	99.9	0.1	0.0	33.0	61.4	755.6
P-K-Mo ₂ C/γ-Al ₂ O ₃ ^[3]	450	2.1	3	1.8	42.1	99.1	0.8	0.2	41.7	7.8	95.5
L-K-Mo ₂ C/γ-Al ₂ O ₃ ^[3]	450	2.1	3	36.7	22.1	97.3	2.0	0.7	21.5	80.0	984.2

References

- [1] J. R. Morse, M. Juneau, J. W. Baldwin, M. D. Porosoff, H. D. Willauer, *Journal of CO₂ Utilization* **2020**, *35*, 38-46.
- [2] W. Xu, P. J. Ramírez, D. Stacchiola, J. L. Brito, J. A. Rodriguez, *Catalysis Letters* **2015**, *145*, 1365-1373.
- [3] M. Juneau, M. Vonglis, J. Hartvigsen, L. Frost, D. Bayerl, M. Dixit, G. Mpourmpakis, J. R. Morse, J. W. Baldwin, H. D. Willauer, M. D. Porosoff, *Energy & Environmental Science* **2020**.